

Using k-means assistant event selection strategy to study anomalous quartic gauge couplings at muon colliders

Shuai Zhang, Ji-Chong Yang,* and Yu-Chen Guo

Department of Physics, Liaoning Normal University, Dalian 116029, China and

Center for Theoretical and Experimental High Energy Physics,

Liaoning Normal University, Dalian 116029, China

(Dated: February 3, 2023)

arXiv:2302.01274v1 [hep-ph] 2 Feb 2023

Abstract

The search for new physics beyond the Standard Model is one of the central problems of current high energy physics interest. As the luminosities of current and near-future colliders continue to increase, the search for new physics has increased the requirements for processing large amounts of data. Mean while, quantum computing which is rapidly evolving, has great potential to become a powerful tool to help search for new physics signals. Since the k-means algorithm is known to be able to be speeded up with the help of quantum computing, we investigate and propose an event selection strategy based on k-means algorithm to search for new physics signals. Taking the case of tri-photon processes at the muon colliders as an example, the event selection strategy is shown to be effective in helping to search for the signal of dimension-8 operators contributing to anomalous quartic gauge couplings.

I. INTRODUCTION

While the Standard Model (SM) has been very successful so far, there are still unanswered questions and the search for new physics (NP) signals beyond the SM is at the forefront of high energy physics (HEP) [1]. On the one hand, except for a few cases known or suspected to deviate from the SM [2–8], there is no clear signal giving guidance for possible NP models. Moreover, the experimental advances in the near decade ahead will be focused on the high luminosity frontier, which makes it important to search for NP efficiently.

A model-independent approach known as the SM effective field theory (SMEFT) has attracted a lot of attention because of its ability to efficiently search for NP signals [9–12]. While the SMEFT is mainly applied to study the dimension-6 operators, dimension-8 operators are getting more and more attention recently [13–18]. The study of the dimension-8 operators is necessary because of the convex geometry perspective to the operator space [19–21]. From a phenomenological point of view, there are many cases where dimension-6 operators are absent, but the dimension-8 operators show up [22–31]. The experiments at the Large Hadron Collider (LHC) also keep a close eye on dimension-8 operators [32–46]. However, for one generation of fermions, there are 895 baryon number conserving dimension-8 operators [13, 47], and kinematic analysis needs to be done for each operator. The efficiency

* yangjichong@lnmu.edu.cn; Corresponding author

decreases with the growth of the number of operators to be considered.

The use of machine learning (ML) algorithms in HEP is recently developing rapidly [48–59]. To further improve efficiency, event selection strategies based on anomaly detection (AD) ML algorithms are introduced to HEP community [60–66]. The strategy to use AD is independent of the operators or NP models to be searched for. Moreover, unlike searching for NP in a process that may turn out to be fruitless, the anomalies found by searching for anomalous signals are always worth attention.

Another promising improvement in efficiency comes from quantum computing [67–69]. It has been shown that, the calculation of distances between two vectors can be accelerated by using the controlled swap gate which is known as swap test [70, 71]. Meanwhile, the calculation of distances is at the core of the famous k-means algorithm [72], and the quantum accelerated k-means algorithms have been developed [73, 74]. The k-means algorithm can also be used for AD, however, whether the k-means AD algorithm (KMAD) is useful in searching for NP is still not known. In this paper, We focus on the feasibility of using KMAD in the search of NP.

As a test bed, we use KMAD to study the dimension-8 anomalous quartic gauge couplings (aQGCs) [75, 76] at the muon colliders. The aQGCs also draw a lot of attention at the LHC because they are closely related to the NP w.r.t. electroweak symmetry breaking [14, 19, 20, 47, 77]. Meanwhile, the muon colliders have received a lot of attention recently due to their abilities to reach both high energies and high luminosities, while keeping cleaner environment less affected by the QCD backgrounds [78–87]. The tri-photon processes at the muon colliders are shown to be sensitive to the transverse operators contributing to the aQGCs [88]. In this paper, we present an event selection strategy to search for the signals of aQGCs and set constraints on the operator coefficients with the help of KMAD.

The rest of this paper is organized as follows. In Sec. II, the dimension-8 operators contributing to aQGCs and the tri-photon process are briefly reviewed. The event selection strategy using KMAD is discussed in Sec. III. The expected constraints on the operator coefficients are presented in Sec. IV. Sec. V summarizes our main conclusions.

coefficient	constraint	coefficient	constraint
f_{T_0}/Λ^4	[-0.12, 0.11] [44]	f_{T_6}/Λ^4	[-0.4, 0.4] [45]
f_{T_1}/Λ^4	[-0.12, 0.13] [44]	f_{T_7}/Λ^4	[-0.9, 0.9] [45]
f_{T_2}/Λ^4	[-0.28, 0.28] [44]	f_{T_8}/Λ^4	[-0.43, 0.43] [46]
f_{T_5}/Λ^4	[-0.5, 0.5] [45]	f_{T_9}/Λ^4	[-0.92, 0.92] [46]

TABLE I. The constraints on the O_{T_i} coefficients obtained at 95% C.L at the LHC.

II. THE CONTRIBUTION OF AQGCs TO THE TRI-PHOTON PROCESS

The frequently used dimension-8 operators contributing to aQGCs can be classified as scalar/longitudinal operators O_{S_i} , mixed transverse and longitudinal operators O_{M_i} and transverse operators O_{T_i} [47]. At tree level, the tri-photon process at muon colliders can be contributed by O_{T_i} operators [75, 76],

$$\begin{aligned}
O_{T,0} &= \text{Tr} \left[\widehat{W}_{\mu\nu} \widehat{W}^{\mu\nu} \right] \times \text{Tr} \left[\widehat{W}_{\alpha\beta} \widehat{W}^{\alpha\beta} \right], & O_{T,1} &= \text{Tr} \left[\widehat{W}_{\alpha\nu} \widehat{W}^{\mu\beta} \right] \times \text{Tr} \left[\widehat{W}_{\mu\beta} \widehat{W}^{\alpha\nu} \right], \\
O_{T,2} &= \text{Tr} \left[\widehat{W}_{\alpha\mu} \widehat{W}^{\mu\beta} \right] \times \text{Tr} \left[\widehat{W}_{\beta\nu} \widehat{W}^{\nu\alpha} \right], & O_{T,5} &= \text{Tr} \left[\widehat{W}_{\mu\nu} \widehat{W}^{\mu\nu} \right] \times B_{\alpha\beta} B^{\alpha\beta}, \\
O_{T,6} &= \text{Tr} \left[\widehat{W}_{\alpha\nu} \widehat{W}^{\mu\beta} \right] \times B_{\mu\beta} B^{\alpha\nu}, & O_{T,7} &= \text{Tr} \left[\widehat{W}_{\alpha\mu} \widehat{W}^{\mu\beta} \right] \times B_{\beta\nu} B^{\nu\alpha}, \\
O_{T,8} &= B_{\mu\nu} B^{\mu\nu} \times B_{\alpha\beta} B^{\alpha\beta}, & O_{T,9} &= B_{\alpha\mu} B^{\mu\beta} \times B_{\beta\nu} B^{\nu\alpha},
\end{aligned} \tag{1}$$

where $\widehat{W} \equiv \vec{\sigma} \cdot \vec{W}/2$ with σ being the Pauli matrices and $\vec{W} = \{W^1, W^2, W^3\}$, B_μ and W_μ^i are $U(1)_Y$ and $SU(2)_I$ gauge fields, and $B_{\mu\nu}$ and $W_{\mu\nu}$ correspond to the gauge invariant field strength tensors. The constraints on the coefficients obtained by the LHC are listed in Table I.

At tree level, there are only two Feynman diagrams induced by O_{T_i} operators as shown on the left panel of Fig. 1. The SM background is shown on the right panel of Fig. 1. For the tri-photon process, the contribution of $O_{T_{1,6}}$ operators are exactly as same as $O_{T_{0,5}}$ operators, respectively. In the following, we concentrate on $O_{T_{0,2,5,7,8,9}}$ operators.

III. K-MEANS ASSISTANT EVENT SELECTION STRATEGY

Typically, the searching of NP at a collider with a high luminosity is to look for a small number of anomalies in the vast amount of data. Meanwhile, AD algorithms are designed

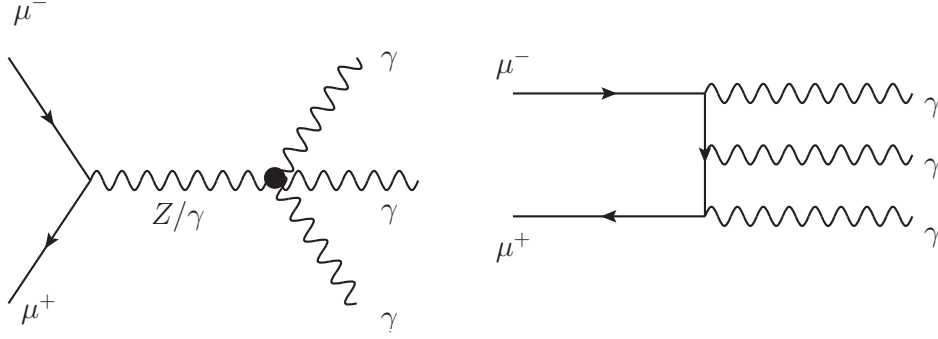


FIG. 1. Feynman diagrams for the tri-photon processes $\mu^+\mu^- \rightarrow \gamma\gamma\gamma$ at the muon colliders. The diagrams induced by O_{T_i} operators are shown in the left panel, and one of the diagrams in the SM is shown in the right panel. In the SM, there are other five diagrams which can be obtained by permuting the photons in the final state.

to search for those events which are ‘few and different’. Therefore, it can be expected that the AD algorithms are suitable to search for NP signals.

In the simplest case, one can assume that the elements in the data-set are Gaussian distributed. The degree of anomaly of each event can be quantified by the distance of the point representing the event from the centroid of all points. However, the picture of Gaussian distribution is often over simplified for the case of searching for NP. As an example, a more complicated case is shown in Fig. 2. The anomalous point is depicted as the black dot, which is approximately at the centroid of all points, therefore, the degree of anomaly can no longer be quantified by the distance of the point from the centroid of all points. On the other hand, as shown in the Fig. 2, the normal points can be divided into three clusters. The anomalous point is far from the centroids of all clusters. The exploitation of this feature is the key idea of KMAD. By using KMAD, we use k-means to find the centroids of the clusters automatically. After clustering, we calculate the distances of the points to the centroids of all clusters. Since the anomalous point is far from all centroids, the distance from a point to the nearest centroid can be used to quantify the degree of anomaly of the point.

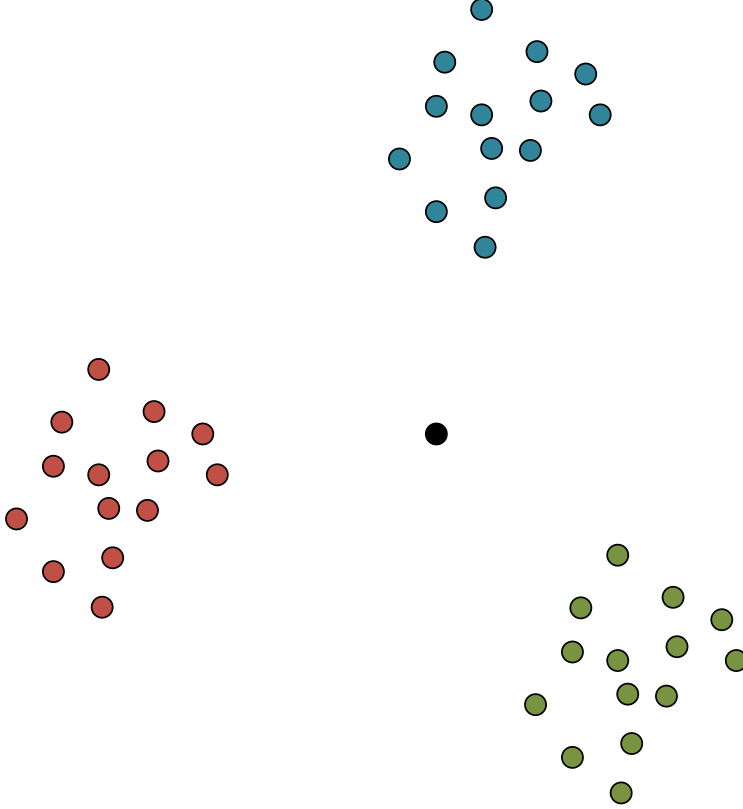


FIG. 2. A demonstration of the search for anomalous signals when the distribution of points is not Gaussian. The black dot in the center is the anomalous point. The blue, red and green points are normal points which can be divided into three clusters. The anomalous point is far away from the centroids of all clusters.

A. Data preparation

To prepare the data-set, we generate the events using Monte Carlo (MC) simulation with the help of `MadGraph5@NLO` toolkit [89–91], including a muon collider-like detector simulation with `Delphes` [92]. To avoid inferred divergences, in this section we use the standard cut as default, the cuts relevant to inferred divergences are

$$p_{T,\gamma} > 10 \text{ GeV}, \quad |\eta_\gamma| < 2.5, \quad \Delta R_{\gamma\gamma} > 0.4, \quad (2)$$

where $p_{T,\gamma}$ and η_γ are the transverse momentum and pseudo-rapidity for each photon, respectively, $\Delta R_{\gamma\gamma} = \sqrt{\Delta\phi^2 + \Delta\eta^2}$ where $\Delta\phi$ and $\Delta\eta$ are difference between the azimuth angles and pseudo-rapidities of two photons. The events for signals are generated with one operator at a time. In this section, the coefficients are chosen as the upper bound of Table I.

As will be introduced later, the coefficients as well as the operators to be searched for are actually irrelevant.

To build data-sets for the KMAD, we require each event to have at least three photons. The data-sets are composed of the 4-momenta of the three hardest photons, i.e., we select three photons with the highest energy and rank them in descending order of energy, taking the components of the 4-momentum of each photon in the order, so that an event can be correspond to a 12-dimensional vector. In this section, we select 600000 events for the SM, and 200000 events are generated for the NP. The interference is ignored in this section.

B. Event selection strategy

The number of clusters in the k-means algorithm is often denoted as the k , and the cluster assignment is often denoted as the k-value. The following is a brief summary of the implementation of KMAD,

1. Specify a k-value for each point randomly.
2. Calculate the cluster centroid as the center of the points with k-values as same as the cluster.
3. Calculate the distance from each point to the k centroids (all centroids) separately, and by comparing the distances, specify the k-value of the point as the k-value of the nearest centroid.
4. Repeat steps 2 and 3, until the k-value of each point is no longer changing.
5. Calculate the anomaly score of one point as the distance (denoted as d) from the point to the centroid with the same k-value as this point.

Denote the number of points whose k-value changed at the previous step as n , practically, to speed up the procedure, we stop when n is less than 0.1% of the total event number. There are cases where the classes corresponding to some k-values are empty. In this case, we divide the the largest cluster randomly and maintain the total number of clusters as k . When the k-means process (step 1 to 4) is finished, we can calculate how anomalous a point is, which is called anomaly score (d in step 4). Since the k-values given in the first step are random,

and we stop before $n = 0$, the results of the distances of the points to the centroids are not fixed. To avoid the effect of these randomness, we repeated the above process m times and make use of the average of the distances (denoted as \bar{d}), i.e. the the average anomaly score to distinguish the signal events from the background events.

If it is to find anomalous signals in a data-set, only the data-set needs to be provided without specifying the source of the data-set, and the physical content behind it. KMAD will automatically discover those anomalous events in the data-set that are different from the majority. Thus KMAD is an unsupervised learning algorithm. At the same time, KMAD can also be used as a supervised learning algorithm. In steps 1-4, the SM data-set obtained from MC can be used, and the process of obtaining centroids can be regarded as the training process. In step 5, the data-set from the experiment is used to find signals in the experimental data-set that are different from the SM.

The difference between the two approaches can be neglected if it is assumed that the number of NP signals is small enough to affect the distribution of centroids. Both approaches do not need to know what the NPs are being searched for, do not require kinematic analysis, and are therefore automatic event selection strategies.

When the second approach is used, the operator coefficients are completely irrelevant if only the distribution characteristics of the anomalous scores are studied. Therefore, in this section we use the second approach. We will use the first approach in the next section.

As introduced, the number of repetitions of the KMAD process m is a tunable parameter. m can be used to control the accuracy of the event selection strategy. We studied the rate of convergence of \bar{d} as m grows. Picking an event from the SM background and O_{T_0} signals at 3 TeV, 10 TeV, 14 TeV and 30 TeV, \bar{d} as functions of m at $k = 50$ are shown in Fig. 3. We find that \bar{d} converges rapidly as m grows, when $m = 200$, the value of \bar{d} starts to become stable. Theoretically, the value of m can continue to increase to make the relative statistical error of \bar{d} smaller, but due to limited compute power, we use $m = 200$ in this paper. The relative statistical error of \bar{d} for each point does not exceed 4%.

Another tunable parameter of KMAD is k . Fig. 4 shows the distribution of the SM and NP anomaly scores at different k . It can be seen that the distributions of the anomaly scores for the SM background and the NP signals are different. When k takes different values, the larger k is, the better the distinguishing. This behavior will be explained in the next subsection. With limited compute power, we take the value of k as 50 in this paper.

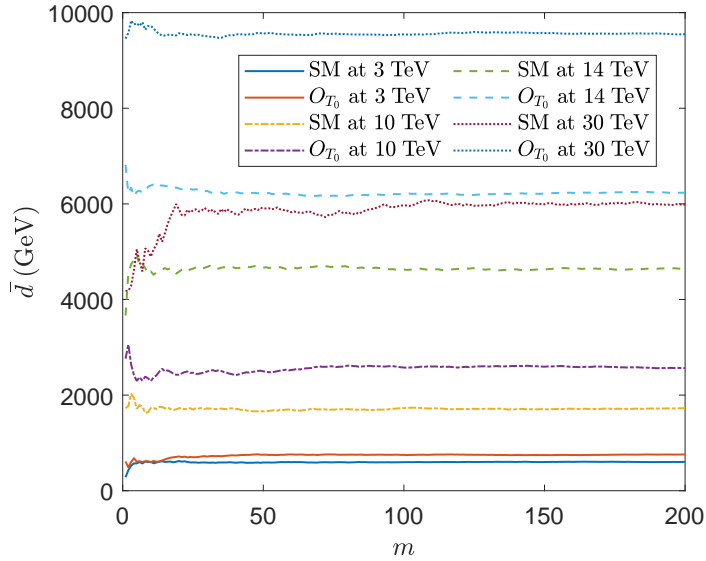


FIG. 3. \bar{d} as functions of m at $k = 50$. We find that \bar{d} converges rapidly as m grows.

C. Why does KMAD work

Before we use the KMAD algorithm to constraint the operator coefficients, there is an interesting question that needs to be explained. Why is KMAD suitable in our case?

Take the hardest photon as an example. If the 3-momentum of the hardest photon is denoted as \mathbf{p}_1 , then p_1^x , p_1^y and p_1^z are roughly distributed over a thick spherical shell with $0.99 \text{ TeV} < E_\gamma < 1.57 \text{ TeV}$, as shown in Fig. 5.

Taking one k-means process for $k = 2, 10, 50$ at $\sqrt{s} = 3 \text{ TeV}$ as examples. The events with different k-values are colored differently. The centroids for different clusters are also shown in Fig. 5, with lattice balls around the centroids. If d is used to distinguish the NP signals from the SM background, in the $p_1^x - p_1^y - p_1^z$ space, it is equivalent to consider the events inside the lattice balls as the SM background and the events outside as the NP signals. In Fig. 5, the radii of the balls for $k = 2, 10, 50$ are 1.2 TeV, 0.8 TeV and 0.5 TeV, respectively. It can be seen that the key for KMAD to work is whether the lattice balls can roughly put together the shape of the distribution of background events. Fig. 5 also shows why larger k is better, because the more balls can sample an arbitrarily shaped distribution more accurately.

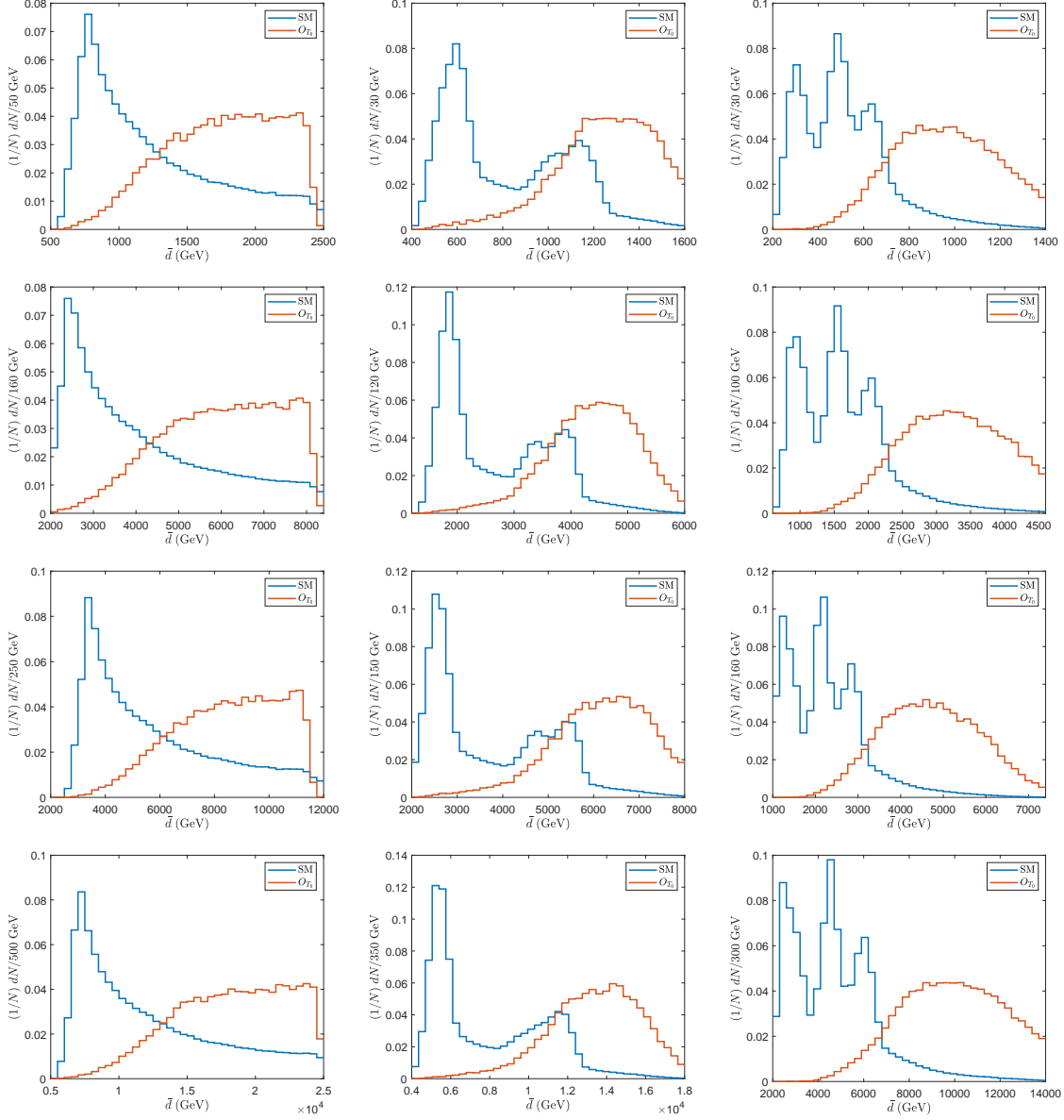


FIG. 4. The normalized distribution of anomaly score \bar{d} when $k = 2$ (column 1), 10 (column 2), and 50 (column 3), at $\sqrt{s} = 3$ TeV (row 1), 10 TeV (row 2), 14 TeV (row 3) and 30 TeV (row 4) for the SM and O_{T_0} induced contribution.

IV. CONSTRAINTS ON THE COEFFICIENTS

When no NP signals are found, the study of NP is to set constraints on the parameters of NP. The KMAD can also be used to set constraints on the coefficients of operators contributing to aQGCs. For this purpose, we generate events by using MC with coefficients

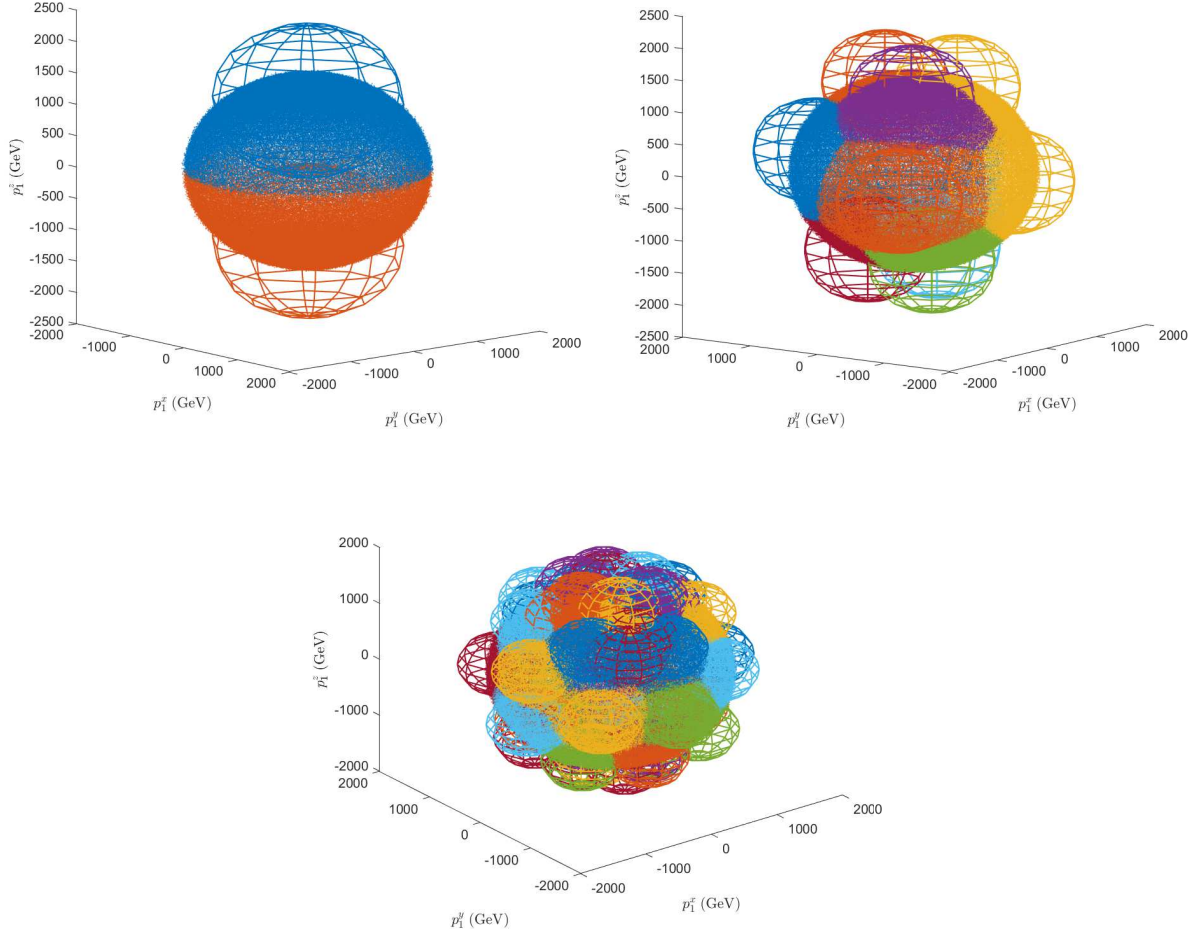


FIG. 5. The distribution of the SM background in the $p_1^x - p_1^y - p_1^z$ space. The events are colored according to the cluster assignments. The centroids of the clusters are also shown, and the lattice balls are drawn with the centroids as the centers of the balls and d as the radii. There are clusters overlap with each other because they are separated in other dimensions.

in Table. II. The contribution of interference between the SM and aQGCs is also included. It has been shown that $p_{T,\gamma}$ provides an efficient cut to suppress the SM background. In Ref. [88], $p_{T,\gamma} > 0.12E_{\text{beam}}$ is used as a part of the event selection strategy where E_{beam} is the energy of the beam. To leave some room for KMAD, when generating events, in the standard cuts $p_{T,\gamma} > 0.1E_{\text{beam}}$ is used, other standard cuts relevant to inferred divergences are as same as those in Eq. (2). Similar as the previous section, at least 3 photons are required to present after fast detector simulation. Then the KMAD event selection strategy is applied to select the events with \bar{d} larger than 700 GeV, 2000 GeV, 3000 GeV and 7000 GeV for $\sqrt{s} = 3$ TeV,

\sqrt{s}	3 TeV	10 TeV	14 TeV	30 TeV
Unit of coefficient	(TeV ⁻⁴)	(10 ⁻³ TeV ⁻⁴)	(10 ⁻³ TeV ⁻⁴)	(10 ⁻⁴ TeV ⁻⁴)
f_{T_0}/Λ^4	[-0.3, 0.3]	[-1.5, 1.5]	[-0.5, 0.5]	[-0.5, 0.5]
f_{T_2}/Λ^4	[-0.5, 0.5]	[-2.0, 2.0]	[-0.8, 0.8]	[-0.8, 0.8]
f_{T_5}/Λ^4	[-0.06, 0.06]	[-0.3, 0.3]	[-0.1, 0.1]	[-0.08, 0.08]
f_{T_7}/Λ^4	[-0.1, 0.1]	[-0.5, 0.5]	[-0.15, 0.15]	[-0.15, 0.15]
f_{T_8}/Λ^4	[-0.01, 0.01]	[-0.05, 0.05]	[-0.015, 0.015]	[-0.015, 0.015]
f_{T_9}/Λ^4	[-0.016, 0.016]	[-0.08, 0.08]	[-0.02, 0.02]	[-0.02, 0.02]

TABLE II. The range of coefficients used in scanning.

10 TeV, 14 TeV and 30 TeV, respectively.

With aQGCs presented, the cross-section of tri-photon process can be written as

$$\sigma = \sigma_{\text{SM}} + \sigma_{\text{int}} f_{T_i}/\Lambda^4 + \sigma_{\text{NP}} (f_{T_i}/\Lambda^4)^2, \quad (3)$$

where σ_{SM} is the SM contribution, $f_{T_i}/\Lambda^4 \sigma_{\text{int}}$ denotes interference between the SM and aQGCs, $\sigma_{\text{NP}} (f_{T_i}/\Lambda^4)^2$ is the aQGCs induced contribution. The analytical results of σ_{int} and σ_{NP} before cuts can be found in Ref. [88]. After event selection strategy, the cross-section is fitted as a bilinear function of f_{T_i}/Λ^4 in Eq. (3). The cross-sections after event selection strategy and the fitted cross-sections are shown in Fig. 6. It can be found from Fig. 6 that after the event selection strategy, the cross-sections still fit bilinear functions well when the coefficients are within the range listed in Table II. The interference between the SM and aQGCs plays an important role in the tri-photon process. From Fig. 6, it can be found that the KMAD works well when the interference presents.

The constraints on the coefficients are estimated by using statistical sensitivity defined as [93, 94]

$$\mathcal{S}_{\text{stat}} = \sqrt{2 [(N_{\text{bg}} + N_s) \ln(1 + N_s/N_{\text{bg}}) - N_s]}, \quad (4)$$

where $N_s = (\sigma - \sigma_{\text{SM}})L$ and $N_{\text{bg}} = \sigma_{\text{SM}}L$, and L is the luminosity. In this paper, the luminosities in both the ‘‘conservative’’ and ‘‘optimistic’’ cases [82] are considered. The constraints on the coefficients at $\mathcal{S}_{\text{stat}} = 2, 3, 5$ are listed in Table III and Table IV.

In this paper, the energies and luminosities are as same as those used in Ref. [88], but with a different event selection strategy. It can be seen from Tables III and IV that, the

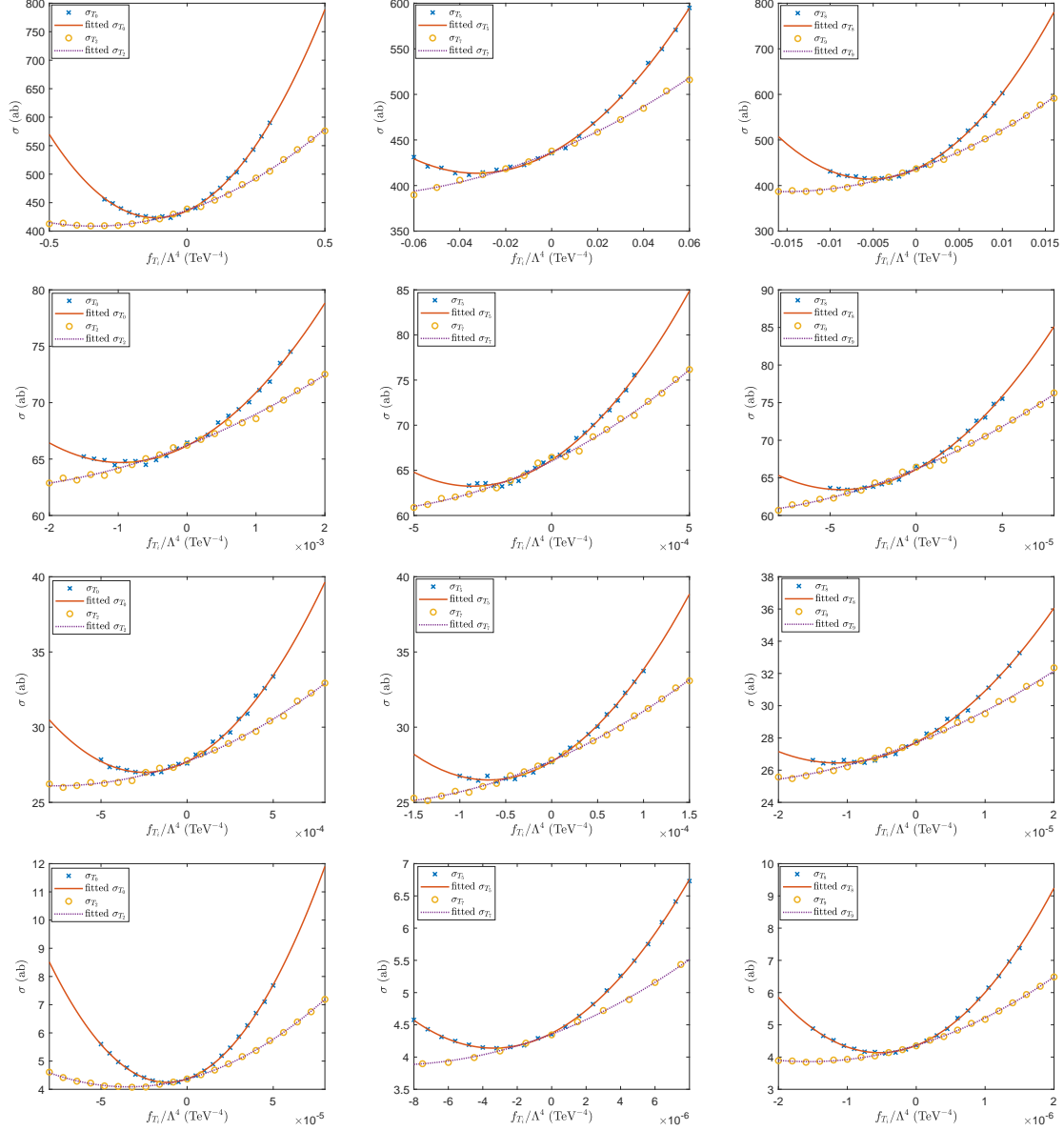


FIG. 6. The cross-sections σ and fitted σ as bilinear functions of f_{T_i}/Λ^4 at $\sqrt{s} = 3$ TeV (row 1), 10 TeV (row 2), 14 TeV (row 3) and 30 TeV (row 4).

upper bounds in this paper are generally about one order of magnitude tighter than those in Ref. [88], the lower bounds are also generally much tighter than those in Ref. [88]. It can be concluded that, the KMAD is useful and efficient in the search of NP signals.

	S_{stat}	3 TeV 1 ab ⁻¹ (10 ⁻² TeV ⁻⁴)	10 TeV 10 ab ⁻¹ (10 ⁻⁴ TeV ⁻⁴)	14 TeV 10 ab ⁻¹ (10 ⁻⁴ TeV ⁻⁴)	30 TeV 10 ab ⁻¹ (10 ⁻⁵ TeV ⁻⁴)
$f_{T_0}(f_{T_1})/\Lambda^4$	2	[-24.17, 1.68]	[-20.43, 1.21]	[-5.60, 0.614]	[-3.48, 1.16]
	3	[-25.97, 3.49]	[-21.76, 2.53]	[-6.21, 1.22]	[-4.29, 1.97]
	5	[-30.48, 7.99]	[-25.18, 5.95]	[-7.62, 2.64]	[-5.78, 3.46]
f_{T_2}/Λ^4	2	[-70.18, 2.34]	[-68.06, 1.62]	[-16.03, 0.877]	[-8.64, 1.80]
	3	[-72.86, 5.01]	[-69.96, 3.52]	[-16.99, 1.83]	[-10.06, 3.22]
	5	[-80.10, 12.26]	[-75.32, 8.87]	[-19.40, 4.25]	[-12.83, 5.98]
$f_{T_5}(f_{T_6})/\Lambda^4$	2	[-6.81, 0.276]	[-5.97, 0.192]	[-1.48, 0.103]	[-0.883, 0.207]
	3	[-7.12, 0.587]	[-6.19, 0.413]	[-1.59, 0.213]	[-1.04, 0.366]
	5	[-7.95, 1.41]	[-6.80, 1.02]	[-1.86, 0.482]	[-1.35, 0.671]
f_{T_7}/Λ^4	2	[-19.38, 0.375]	[-15.04, 0.258]	[-4.52, 0.142]	[-2.20, 0.312]
	3	[-19.82, 0.816]	[-15.35, 0.565]	[-4.68, 0.304]	[-2.47, 0.580]
	5	[-21.07, 2.06]	[-16.24, 1.45]	[-5.11, 0.738]	[-3.01, 1.12]
f_{T_8}/Λ^4	2	[-1.10, 0.0445]	[-0.901, 0.0310]	[-0.246, 0.0165]	[-0.139, 0.0332]
	3	[-1.15, 0.0948]	[-0.936, 0.0667]	[-0.263, 0.0341]	[-0.165, 0.0587]
	5	[-1.28, 0.228]	[-1.03, 0.164]	[-0.307, 0.0776]	[-0.213, 0.107]
f_{T_9}/Λ^4	2	[-3.13, 0.0600]	[-2.62, 0.0412]	[-0.646, 0.0227]	[-0.362, 0.0493]
	3	[-3.20, 0.131]	[-2.66, 0.0903]	[-0.672, 0.0482]	[-0.404, 0.0921]
	5	[-3.40, 0.330]	[-2.81, 0.233]	[-0.739, 0.116]	[-0.492, 0.179]

TABLE III. The projected sensitivities on the coefficients of the O_{T_i} operators at the muon colliders with different c.m. energies and integrated luminosities for the “conservative” case.

V. SUMMARY

Searching for NP signals requires processing a large amount of data, while it has been shown that the k-means algorithm is able to be accelerated by using quantum computers, which are capable of handling large amounts of data, so it is a question worth investigating whether the k-means algorithm can also be used to search for NP signals. In this paper, taking the case of aQGCs in the tri-photon processes at the muon colliders as an example, we

	S_{stat}	14 TeV 20 ab ⁻¹ (10 ⁻⁵ TeV ⁻⁴)	30 TeV 90 ab ⁻¹ (10 ⁻⁶ TeV ⁻⁴)
$f_{T_0}(f_{T_1})/\Lambda^4$	2	[-53.09, 3.26]	[-25.12, 1.92]
	3	[-56.64, 6.81]	[-27.15, 3.95]
	5	[-65.72, 15.89]	[-32.14, 8.95]
f_{T_2}/Λ^4	2	[-156.10, 4.53]	[-71.03, 2.60]
	3	[-161.35, 9.78]	[-73.99, 5.56]
	5	[-175.86, 24.30]	[-81.90, 13.47]
$f_{T_5}(f_{T_6})/\Lambda^4$	2	[-14.27, 0.538]	[-7.06, 0.308]
	3	[-14.88, 1.15]	[-7.41, 0.653]
	5	[-16.54, 2.80]	[-8.32, 1.56]
f_{T_7}/Λ^4	2	[-44.47, 0.728]	[-19.30, 0.423]
	3	[-45.34, 1.59]	[-19.79, 0.918]
	5	[-47.83, 4.09]	[-21.17, 2.30]
f_{T_8}/Λ^4	2	[-2.38, 0.0860]	[-1.11, 0.0497]
	3	[-2.48, 0.184]	[-1.17, 0.105]
	5	[-2.74, 0.450]	[-1.31, 0.251]
f_{T_9}/Λ^4	2	[-6.35, 0.116]	[-3.19, 0.0666]
	3	[-6.49, 0.253]	[-3.27, 0.145]
	5	[-6.88, 0.647]	[-3.49, 0.363]

TABLE IV. Same as Table III but for the “optimistic” case.

propose an event selection strategy using KMAD which is based on the k-means algorithm to search for NP signals.

By using MC, the expected constraints on the coefficients of the operators contributing to aQGCs are calculated. The upper bounds in this paper are generally about one order of magnitude tighter than those obtained by using a traditional event selection strategy. Apart from that, as an anomaly detection algorithm KMAD is an automatic event selection strategy that does not require kinematic analysis. Moreover, KMAD does not require knowing what the NP is to be searched for if the purpose is to looking for anomalous signals. It can be

concluded that, the KMAD is useful and efficient in the search of NP signals.

The ability of quantum computing to handle large amounts of data will provide a whole new opportunity in the study of NP. Since the k-means algorithm can be accelerated by quantum computing and, at the same time, the k-means algorithm can be used to search for NP signals, we expect that the quantum computers can be used to help to search for NP in the near future.

ACKNOWLEDGMENTS

This work was supported in part by the National Natural Science Foundation of China under Grants Nos. 11905093 and 12147214, the Natural Science Foundation of the Liaoning Scientific Committee No. LJKZ0978 and the Outstanding Research Cultivation Program of Liaoning Normal University (No.21GDL004).

-
- [1] J. Ellis, Outstanding questions: Physics beyond the Standard Model, *Phil. Trans. Roy. Soc. Lond. A* **370**, 818 (2012).
 - [2] O. Cremonesi, Neutrino masses and Neutrinoless Double Beta Decay: Status and expectations (2010) arXiv:1002.1437 [hep-ex].
 - [3] A. de Gouvea, A. Friedland, P. Huber, and I. Mocioiu, *Community Summer Study 2013: Snowmass on the Mississippi* (2013) arXiv:1309.7338 [hep-ph].
 - [4] G. W. Bennett, B. Bousquet, H. N. Brown, G. Bunce, R. M. Carey, P. Cushman, G. T. Danby, P. T. Debevec, M. Deile, H. Deng, W. Deninger, S. K. Dhawan, V. P. Druzhinin, L. Duong, E. Efstathiadis, F. J. M. Farley, G. V. Fedotovitch, S. Giron, F. E. Gray, D. Grigoriev, M. Grosse-Perdekamp, A. Grossmann, M. F. Hare, D. W. Hertzog, X. Huang, V. W. Hughes, M. Iwasaki, K. Jungmann, D. Kawall, M. Kawamura, B. I. Khazin, J. Kindem, F. Krienen, I. Kronkvist, A. Lam, R. Larsen, Y. Y. Lee, I. Logashenko, R. McNabb, W. Meng, J. Mi, J. P. Miller, Y. Mizumachi, W. M. Morse, D. Nikas, C. J. G. Onderwater, Y. Orlov, C. S. Özben, J. M. Paley, Q. Peng, C. C. Polly, J. Pretz, R. Prigl, G. zu Putlitz, T. Qian, S. I. Redin, O. Rind, B. L. Roberts, N. Ryskulov, S. Sedykh, Y. K. Semertzidis, P. Shagin, Y. M. Shatunov, E. P. Sichtermann, E. Solodov, M. Sossong, A. Steinmetz, L. R. Sulak, C. Tim-

- mermans, A. Trofimov, D. Urner, P. von Walter, D. Warburton, D. Winn, A. Yamamoto, and D. Zimmerman (Muon g-2 Collaboration), Final report of the e821 muon anomalous magnetic moment measurement at bnl, *Phys. Rev. D* **73**, 072003 (2006).
- [5] S. Descotes-Genon, L. Hofer, J. Matias, and J. Virto, Global analysis of $b \rightarrow s\ell\ell$ anomalies, *JHEP* **06**, 092, arXiv:1510.04239 [hep-ph].
- [6] R. Aaij *et al.* (LHCb), Test of lepton universality using $B^+ \rightarrow K^+\ell^+\ell^-$ decays, *Phys. Rev. Lett.* **113**, 151601 (2014), arXiv:1406.6482 [hep-ex].
- [7] M. Huschle *et al.* (Belle), Measurement of the branching ratio of $\bar{B} \rightarrow D^{(*)}\tau^-\bar{\nu}_\tau$ relative to $\bar{B} \rightarrow D^{(*)}\ell^-\bar{\nu}_\ell$ decays with hadronic tagging at Belle, *Phys. Rev. D* **92**, 072014 (2015), arXiv:1507.03233 [hep-ex].
- [8] T. Aaltonen *et al.* (CDF), High-precision measurement of the W boson mass with the CDF II detector, *Science* **376**, 170 (2022).
- [9] S. Weinberg, Baryon and Lepton Nonconserving Processes, *Phys. Rev. Lett.* **43**, 1566 (1979).
- [10] B. Grzadkowski, M. Iskrzynski, M. Misiak, and J. Rosiek, Dimension-Six Terms in the Standard Model Lagrangian, *JHEP* **10**, 085, arXiv:1008.4884 [hep-ph].
- [11] S. Willenbrock and C. Zhang, Effective Field Theory Beyond the Standard Model, *Ann. Rev. Nucl. Part. Sci.* **64**, 83 (2014), arXiv:1401.0470 [hep-ph].
- [12] E. Masso, An Effective Guide to Beyond the Standard Model Physics, *JHEP* **10**, 128, arXiv:1406.6376 [hep-ph].
- [13] B. Henning, X. Lu, T. Melia, and H. Murayama, 2, 84, 30, 993, 560, 15456, 11962, 261485, ...: Higher dimension operators in the SM EFT, *JHEP* **08**, 016, [Erratum: *JHEP* 09, 019 (2019)], arXiv:1512.03433 [hep-ph].
- [14] D. R. Green, P. Meade, and M.-A. Pleier, Multiboson interactions at the LHC, *Rev. Mod. Phys.* **89**, 035008 (2017), arXiv:1610.07572 [hep-ex].
- [15] G. Perez, M. Sekulla, and D. Zeppenfeld, Anomalous quartic gauge couplings and unitarization for the vector boson scattering process $pp \rightarrow W^+W^+jjX \rightarrow \ell^+\nu_\ell\ell^+\nu_\ell jjX$, *Eur. Phys. J. C* **78**, 759 (2018), arXiv:1807.02707 [hep-ph].
- [16] Y.-C. Guo, Y.-Y. Wang, J.-C. Yang, and C.-X. Yue, Constraints on anomalous quartic gauge couplings via $W\gamma jj$ production at the LHC, *Chin. Phys. C* **44**, 123105 (2020), arXiv:2002.03326 [hep-ph].
- [17] Y.-C. Guo, Y.-Y. Wang, and J.-C. Yang, Constraints on anomalous quartic gauge couplings

- by $\gamma\gamma \rightarrow W^+W^-$ scattering, Nucl. Phys. B **961**, 115222 (2020), arXiv:1912.10686 [hep-ph].
- [18] J.-C. Yang, Y.-C. Guo, C.-X. Yue, and Q. Fu, Constraints on anomalous quartic gauge couplings via $Z\gamma jj$ production at the LHC, Phys. Rev. D **104**, 035015 (2021), arXiv:2107.01123 [hep-ph].
- [19] C. Zhang and S.-Y. Zhou, Positivity bounds on vector boson scattering at the LHC, Phys. Rev. D **100**, 095003 (2019), arXiv:1808.00010 [hep-ph].
- [20] Q. Bi, C. Zhang, and S.-Y. Zhou, Positivity constraints on aQGC: carving out the physical parameter space, JHEP **06**, 137, arXiv:1902.08977 [hep-ph].
- [21] C. Zhang and S.-Y. Zhou, Convex Geometry Perspective to the (Standard Model) Effective Field Theory Space, Phys. Rev. Lett. **125**, 201601 (2020), arXiv:2005.03047 [hep-ph].
- [22] M. Born and L. Infeld, Foundations of the new field theory, Proc. Roy. Soc. Lond. A **144**, 425 (1934).
- [23] J. Ellis and S.-F. Ge, Constraining Gluonic Quartic Gauge Coupling Operators with $gg \rightarrow \gamma\gamma$, Phys. Rev. Lett. **121**, 041801 (2018), arXiv:1802.02416 [hep-ph].
- [24] J. Ellis, N. E. Mavromatos, and T. You, Light-by-Light Scattering Constraint on Born-Infeld Theory, Phys. Rev. Lett. **118**, 261802 (2017), arXiv:1703.08450 [hep-ph].
- [25] C. Degrande, A basis of dimension-eight operators for anomalous neutral triple gauge boson interactions, JHEP **02**, 101, arXiv:1308.6323 [hep-ph].
- [26] J. Ellis, S.-F. Ge, H.-J. He, and R.-Q. Xiao, Probing the scale of new physics in the $ZZ\gamma$ coupling at e^+e^- colliders, Chin. Phys. C **44**, 063106 (2020), arXiv:1902.06631 [hep-ph].
- [27] J. Ellis, H.-J. He, and R.-Q. Xiao, Probing new physics in dimension-8 neutral gauge couplings at e^+e^- colliders, Sci. China Phys. Mech. Astron. **64**, 221062 (2021), arXiv:2008.04298 [hep-ph].
- [28] G. J. Gounaris, J. Layssac, and F. M. Renard, Off-shell structure of the anomalous Z and γ selfcouplings, Phys. Rev. D **62**, 073012 (2000), arXiv:hep-ph/0005269.
- [29] G. J. Gounaris, J. Layssac, and F. M. Renard, Signatures of the anomalous Z_γ and ZZ production at the lepton and hadron colliders, Phys. Rev. D **61**, 073013 (2000), arXiv:hep-ph/9910395.
- [30] A. Senol, H. Denizli, A. Yilmaz, I. Turk Cakir, K. Y. Oyulmaz, O. Karadeniz, and O. Cakir, Probing the Effects of Dimension-eight Operators Describing Anomalous Neutral Triple Gauge Boson Interactions at FCC-hh, Nucl. Phys. B **935**, 365 (2018), arXiv:1805.03475 [hep-ph].

- [31] Q. Fu, J.-C. Yang, C.-X. Yue, and Y.-C. Guo, The study of neutral triple gauge couplings in the process $e^+e^- \rightarrow Z\gamma$ including unitarity bounds, Nucl. Phys. B **972**, 115543 (2021), arXiv:2102.03623 [hep-ph].
- [32] G. Aad *et al.* (ATLAS), Evidence for Electroweak Production of $W^\pm W^\pm jj$ in pp Collisions at $\sqrt{s} = 8$ TeV with the ATLAS Detector, Phys. Rev. Lett. **113**, 141803 (2014), arXiv:1405.6241 [hep-ex].
- [33] A. M. Sirunyan *et al.* (CMS), Measurements of production cross sections of WZ and same-sign WW boson pairs in association with two jets in proton-proton collisions at $\sqrt{s} = 13$ TeV, Phys. Lett. B **809**, 135710 (2020), arXiv:2005.01173 [hep-ex].
- [34] M. Aaboud *et al.* (ATLAS), Studies of $Z\gamma$ production in association with a high-mass dijet system in pp collisions at $\sqrt{s} = 8$ TeV with the ATLAS detector, JHEP **07**, 107, arXiv:1705.01966 [hep-ex].
- [35] V. Khachatryan *et al.* (CMS), Measurement of the cross section for electroweak production of $Z\gamma$ in association with two jets and constraints on anomalous quartic gauge couplings in proton-proton collisions at $\sqrt{s} = 8$ TeV, Phys. Lett. B **770**, 380 (2017), arXiv:1702.03025 [hep-ex].
- [36] A. M. Sirunyan *et al.* (CMS), Measurement of the cross section for electroweak production of a Z boson, a photon and two jets in proton-proton collisions at $\sqrt{s} = 13$ TeV and constraints on anomalous quartic couplings, JHEP **06**, 076, arXiv:2002.09902 [hep-ex].
- [37] V. Khachatryan *et al.* (CMS), Measurement of electroweak-induced production of $W\gamma$ with two jets in pp collisions at $\sqrt{s} = 8$ TeV and constraints on anomalous quartic gauge couplings, JHEP **06**, 106, arXiv:1612.09256 [hep-ex].
- [38] A. M. Sirunyan *et al.* (CMS), Measurement of vector boson scattering and constraints on anomalous quartic couplings from events with four leptons and two jets in proton-proton collisions at $\sqrt{s} = 13$ TeV, Phys. Lett. B **774**, 682 (2017), arXiv:1708.02812 [hep-ex].
- [39] A. M. Sirunyan *et al.* (CMS), Measurement of differential cross sections for Z boson pair production in association with jets at $\sqrt{s} = 8$ and 13 TeV, Phys. Lett. B **789**, 19 (2019), arXiv:1806.11073 [hep-ex].
- [40] M. Aaboud *et al.* (ATLAS), Observation of electroweak $W^\pm Z$ boson pair production in association with two jets in pp collisions at $\sqrt{s} = 13$ TeV with the ATLAS detector, Phys. Lett. B **793**, 469 (2019), arXiv:1812.09740 [hep-ex].

- [41] A. M. Sirunyan *et al.* (CMS), Measurement of electroweak WZ boson production and search for new physics in WZ + two jets events in pp collisions at $\sqrt{s} = 13\text{TeV}$, Phys. Lett. B **795**, 281 (2019), arXiv:1901.04060 [hep-ex].
- [42] V. Khachatryan *et al.* (CMS), Evidence for exclusive $\gamma\gamma \rightarrow W^+W^-$ production and constraints on anomalous quartic gauge couplings in pp collisions at $\sqrt{s} = 7$ and 8 TeV, JHEP **08**, 119, arXiv:1604.04464 [hep-ex].
- [43] A. M. Sirunyan *et al.* (CMS), Observation of electroweak production of same-sign W boson pairs in the two jet and two same-sign lepton final state in proton-proton collisions at $\sqrt{s} = 13$ TeV, Phys. Rev. Lett. **120**, 081801 (2018), arXiv:1709.05822 [hep-ex].
- [44] A. M. Sirunyan *et al.* (CMS), Search for anomalous electroweak production of vector boson pairs in association with two jets in proton-proton collisions at 13 TeV, Phys. Lett. B **798**, 134985 (2019), arXiv:1905.07445 [hep-ex].
- [45] A. M. Sirunyan *et al.* (CMS), Observation of electroweak production of $W\gamma$ with two jets in proton-proton collisions at $\sqrt{s} = 13$ TeV, Phys. Lett. B **811**, 135988 (2020), arXiv:2008.10521 [hep-ex].
- [46] A. M. Sirunyan *et al.* (CMS), Evidence for electroweak production of four charged leptons and two jets in proton-proton collisions at $\sqrt{s} = 13$ TeV, Phys. Lett. B **812**, 135992 (2021), arXiv:2008.07013 [hep-ex].
- [47] C. Anders *et al.*, Vector boson scattering: Recent experimental and theory developments, Rev. Phys. **3**, 44 (2018), arXiv:1801.04203 [hep-ph].
- [48] A. Radovic, M. Williams, D. Rousseau, M. Kagan, D. Bonacorsi, A. Himmel, A. Aurisano, K. Terao, and T. Wongjirad, Machine learning at the energy and intensity frontiers of particle physics, Nature **560**, 41 (2018).
- [49] P. Baldi, P. Sadowski, and D. Whiteson, Searching for Exotic Particles in High-Energy Physics with Deep Learning, Nature Commun. **5**, 4308 (2014), arXiv:1402.4735 [hep-ph].
- [50] J. Ren, L. Wu, J. M. Yang, and J. Zhao, Exploring supersymmetry with machine learning, Nucl. Phys. B **943**, 114613 (2019), arXiv:1708.06615 [hep-ph].
- [51] M. Abdughani, J. Ren, L. Wu, and J. M. Yang, Probing stop pair production at the LHC with graph neural networks, JHEP **08**, 055, arXiv:1807.09088 [hep-ph].
- [52] R. Iten, T. Metger, H. Wilming, L. del Rio, and R. Renner, Discovering physical concepts with neural networks, Phys. Rev. Lett. **124**, 010508 (2020).

- [53] J. Ren, L. Wu, and J. M. Yang, Unveiling CP property of top-Higgs coupling with graph neural networks at the LHC, *Phys. Lett. B* **802**, 135198 (2020), arXiv:1901.05627 [hep-ph].
- [54] Y.-C. Guo, L. Jiang, and J.-C. Yang, Detecting anomalous quartic gauge couplings using the isolation forest machine learning algorithm, *Phys. Rev. D* **104**, 035021 (2021), arXiv:2103.03151 [hep-ph].
- [55] M. A. Md Ali, N. Badrud'din, H. Abdullah, and F. Kemi, Alternate methods for anomaly detection in high-energy physics via semi-supervised learning, *Int. J. Mod. Phys. A* **35**, 2050131 (2020).
- [56] E. Fol, R. Tomás, J. Coello de Portugal, and G. Franchetti, Detection of faulty beam position monitors using unsupervised learning, *Phys. Rev. Accel. Beams* **23**, 102805 (2020).
- [57] R. T. D'Agnolo and A. Wulzer, Learning New Physics from a Machine, *Phys. Rev. D* **99**, 015014 (2019), arXiv:1806.02350 [hep-ph].
- [58] J.-C. Yang, X.-Y. Han, Z.-B. Qin, T. Li, and Y.-C. Guo, Measuring the anomalous quartic gauge couplings in the $W^+W^- \rightarrow W^+W^-$ process at muon collider using artificial neural networks, *JHEP* **09**, 074, arXiv:2204.10034 [hep-ph].
- [59] J.-C. Yang, J.-H. Chen, and Y.-C. Guo, Extract the energy scale of anomalous $\gamma\gamma \rightarrow W^+W^-$ scattering in the vector boson scattering process using artificial neural networks, *JHEP* **21**, 085, arXiv:2107.13624 [hep-ph].
- [60] G. Kasieczka *et al.*, The LHC Olympics 2020 a community challenge for anomaly detection in high energy physics, *Rept. Prog. Phys.* **84**, 124201 (2021), arXiv:2101.08320 [hep-ph].
- [61] M. Kuusela, T. Vatanen, E. Malmi, T. Raiko, T. Aaltonen, and Y. Nagai, Semi-Supervised Anomaly Detection - Towards Model-Independent Searches of New Physics, *J. Phys. Conf. Ser.* **368**, 012032 (2012), arXiv:1112.3329 [physics.data-an].
- [62] M. Farina, Y. Nakai, and D. Shih, Searching for New Physics with Deep Autoencoders, *Phys. Rev. D* **101**, 075021 (2020), arXiv:1808.08992 [hep-ph].
- [63] O. Cerri, T. Q. Nguyen, M. Pierini, M. Spiropulu, and J.-R. Vlimant, Variational Autoencoders for New Physics Mining at the Large Hadron Collider, *JHEP* **05**, 036, arXiv:1811.10276 [hep-ex].
- [64] J.-C. Yang, Y.-C. Guo, and L.-H. Cai, Using a nested anomaly detection machine learning algorithm to study the neutral triple gauge couplings at an e^+e^- collider, *Nucl. Phys. B* **977**, 115735 (2022), arXiv:2111.10543 [hep-ph].

- [65] M. van Beekveld, S. Caron, L. Hendriks, P. Jackson, A. Leinweber, S. Otten, R. Patrick, R. Ruiz De Austri, M. Santoni, and M. White, Combining outlier analysis algorithms to identify new physics at the LHC, *JHEP* **09**, 024, arXiv:2010.07940 [hep-ph].
- [66] M. Crispim Romão, N. F. Castro, and R. Pedro, Finding New Physics without learning about it: Anomaly Detection as a tool for Searches at Colliders, *Eur. Phys. J. C* **81**, 27 (2021), arXiv:2006.05432 [hep-ph].
- [67] S. L. Wu *et al.*, Application of quantum machine learning using the quantum kernel algorithm on high energy physics analysis at the LHC, *Phys. Rev. Res.* **3**, 033221 (2021), arXiv:2104.05059 [quant-ph].
- [68] C. W. Bauer *et al.*, Quantum Simulation for High Energy Physics (2022) arXiv:2204.03381 [quant-ph].
- [69] M. S. Alam *et al.*, Quantum computing hardware for HEP algorithms and sensing, in *2022 Snowmass Summer Study* (2022) arXiv:2204.08605 [quant-ph].
- [70] D. Gottesman and I. Chuang, Quantum Digital Signatures (2001) arXiv:quant-ph/0105032 [quant-ph].
- [71] H. Buhrman, R. Cleve, J. Watrous, and R. de Wolf, Quantum fingerprinting, *Phys. Rev. Lett.* **87**, 167902 (2001).
- [72] S. P. Lloyd, Least squares quantization in pcm, *IEEE Trans. Inf. Theory* **28**, 129 (1982).
- [73] S. Lloyd, M. Mohseni, and P. Rebentrost, Quantum algorithms for supervised and unsupervised machine learning (2013) arXiv:1307.0411 [quant-ph].
- [74] I. Kerenidis, J. Landman, A. Luongo, and A. Prakash, Q-means: A quantum algorithm for unsupervised machine learning, in *Proceedings of the 33rd International Conference on Neural Information Processing Systems* (Curran Associates Inc., Red Hook, NY, USA, 2019).
- [75] O. Eboli, M. Gonzalez-Garcia, and J. Mizukoshi, $pp \rightarrow jje^\pm \mu^\pm \nu\nu$ and $jje^\pm \mu^\mp \nu\nu$ at $\mathcal{O}(\alpha_\pm^6)$ and $\mathcal{O}(\alpha_\pm^4 \alpha_s^2)$ for the study of the quartic electroweak gauge boson vertex at CERN LHC, *Phys. Rev. D* **74**, 073005 (2006), arXiv:hep-ph/0606118.
- [76] O. J. P. Éboli and M. C. Gonzalez-Garcia, Classifying the bosonic quartic couplings, *Phys. Rev. D* **93**, 093013 (2016), arXiv:1604.03555 [hep-ph].
- [77] J. Chang, K. Cheung, C.-T. Lu, and T.-C. Yuan, WW scattering in the era of post-Higgs-boson discovery, *Phys. Rev. D* **87**, 093005 (2013), arXiv:1303.6335 [hep-ph].
- [78] D. Buttazzo, D. Redigolo, F. Sala, and A. Tesi, Fusing Vectors into Scalars at High Energy

- Lepton Colliders, *JHEP* **11**, 144, arXiv:1807.04743 [hep-ph].
- [79] J. P. Delahaye, M. Diemoz, K. Long, B. Mansoulié, N. Pastrone, L. Rivkin, D. Schulte, A. Skrinsky, and A. Wulzer, *Muon Colliders* (2019), arXiv:1901.06150 [physics.acc-ph].
- [80] A. Costantini, F. De Lillo, F. Maltoni, L. Mantani, O. Mattelaer, R. Ruiz, and X. Zhao, Vector boson fusion at multi-TeV muon colliders, *JHEP* **09**, 080, arXiv:2005.10289 [hep-ph].
- [81] M. Lu, A. M. Levin, C. Li, A. Agapitos, Q. Li, F. Meng, S. Qian, J. Xiao, and T. Yang, The physics case for an electron-muon collider, *Adv. High Energy Phys.* **2021**, 6693618 (2021), arXiv:2010.15144 [hep-ph].
- [82] H. Al Ali *et al.*, The muon Smasher’s guide, *Rept. Prog. Phys.* **85**, 084201 (2022), arXiv:2103.14043 [hep-ph].
- [83] R. Franceschini and M. Greco, Higgs and BSM Physics at the Future Muon Collider, *Symmetry* **13**, 851 (2021), arXiv:2104.05770 [hep-ph].
- [84] R. Palmer *et al.*, Muon collider design, *Nucl. Phys. B Proc. Suppl.* **51**, 61 (1996), arXiv:acc-phys/9604001.
- [85] S. D. Holmes and V. D. Shiltsev, Muon Collider, in *Outlook for the Future*, edited by C. Joshi, A. Caldwell, P. Muggli, S. D. Holmes, and V. D. Shiltsev (Springer-Verlag Berlin Heidelberg, Germany, 2013) pp. 816–822, arXiv:1202.3803 [physics.acc-ph].
- [86] W. Liu and K.-P. Xie, Probing electroweak phase transition with multi-TeV muon colliders and gravitational waves, *JHEP* **04**, 015, arXiv:2101.10469 [hep-ph].
- [87] W. Liu, K.-P. Xie, and Z. Yi, Testing leptogenesis at the LHC and future muon colliders: A Z' scenario, *Phys. Rev. D* **105**, 095034 (2022), arXiv:2109.15087 [hep-ph].
- [88] J.-C. Yang, Z.-B. Qing, X.-Y. Han, Y.-C. Guo, and T. Li, Tri-photon at muon collider: a new process to probe the anomalous quartic gauge couplings, *JHEP* **22**, 053, arXiv:2204.08195 [hep-ph].
- [89] J. Alwall, R. Frederix, S. Frixione, V. Hirschi, F. Maltoni, O. Mattelaer, H. S. Shao, T. Stelzer, P. Torrielli, and M. Zaro, The automated computation of tree-level and next-to-leading order differential cross sections, and their matching to parton shower simulations, *JHEP* **07**, 079, arXiv:1405.0301 [hep-ph].
- [90] N. D. Christensen and C. Duhr, FeynRules - Feynman rules made easy, *Comput. Phys. Commun.* **180**, 1614 (2009), arXiv:0806.4194 [hep-ph].
- [91] C. Degrande, C. Duhr, B. Fuks, D. Grellscheid, O. Mattelaer, and T. Reiter,

- UFO - The Universal FeynRules Output, *Comput. Phys. Commun.* **183**, 1201 (2012), arXiv:1108.2040 [hep-ph].
- [92] J. de Favereau, C. Delaere, P. Demin, A. Giammanco, V. Lemaître, A. Mertens, and M. Selvaggi (DELPHES 3), DELPHES 3, A modular framework for fast simulation of a generic collider experiment, *JHEP* **02**, 057, arXiv:1307.6346 [hep-ex].
- [93] G. Cowan, K. Cranmer, E. Gross, and O. Vitells, Asymptotic formulae for likelihood-based tests of new physics, *Eur. Phys. J. C* **71**, 1554 (2011), [Erratum: *Eur.Phys.J.C* **73**, 2501 (2013)], arXiv:1007.1727 [physics.data-an].
- [94] P. Zyla *et al.* (Particle Data Group), Review of Particle Physics, *PTEP* **2020**, 083C01 (2020).